J. Astron. Space Sci. 13(1), 32–39 (1996)

PHOSPHINE AND JUPITER'S GREAT RED SPOT

Kim Sang Joon
Kyung Hee Observatory
Department of Astronomy and Space Science
Kyung Hee University, Yong-In, Kyung-Gi-Do
e-mail: sjkim@khobs.kyunghee.ac.kr

(Received April 30, 1996; Accepted May 16, 1996)

ABSTRACT

Voyager IRIS (Infrared Interferometer Spectrometer) observations of Jupiter's Great Red Spot (GRS) have been examined in order to extract the vertical distribution of phosphine. To the accuracy that can be achieved from this approach, there appears to be no difference between the PH_3 distribution over the GRS compared with the distribution over the neighboring South Tropical Zone. This result is at variance with a pre-Voyager prediction of an enhancement of PH_3 over the GRS resulting in the preferential production of red phosphorous in this location on the planet (Prinn & Lewis 1975). The composition of the red material remains an open question.

1. INTRODUCTION

The nature of the chromophore(s) responsible for the color of Jupiter's Great Red Spot (GRS) remains an unsolved problem in the wake of the Galileo encounter. In the last 27 years, two candidates have received special support: carbon-based compounds (Woeller & Ponnamperuma 1969, Khare & Sagan 1973) & red phosphorous - P_4 (Prinn & Lewis 1975). Lewis & Prinn (1970) also suggested that elemental sulfur and ammonium- and hydrogen-polysulfides are responsible for the brown and yellow colors observed various places on the planet's disk. Since Noy *et al.* (1981) have shown that yellow particles can produce a red color on Jupiter under the right conditions, sulfur compounds are also a contender (e.g. Huntress & Anicich 1984). Each of these suggestions carries with it in principle the possibility of an experimental test, but there have been no reports of discrete absorptions that could serve as spectral signatures of the red material in any observations of the GRS to date.

An alternative method for attacking the problem is to look for indications of anomalous concentrations of the precursor materials in the vicinity of the GRS. Both methane and ammonia actually seem deficient over the GRS, but this effect has been successfully interpreted in terms of a high altitude for the GRS cloud material (Owen & Mason 1969, Moroz & Cruikshank 1969, West & Tomasko 1980). No sulfur compound has yet been unambiguously identified on Jupiter, so there is no direct way to monitor the chemistry of this constituent. But phosphine has been detected (Ridgway *et al.* 1976) and the proposal for red phosphorous as the GRS chromophore includes a

specific prediction for the distribution of phosphine over the GRS (Prinn & Lewis 1975). These authors argue that the GRS is a region of strong upward mixing, causing the PH_3 number density to be several orders of magnitude higher at P = 25 mb over the GRS than it is elsewhere on the planet at the same altitude, and in their model, PH_3/H_2 drops precipitously at P = 80 mb, except over the GRS.

Tokunaga *et al.* (1980), using ground-based observations of the planet and a pre-Voyager model for the thermal structure, found no evidence for the strong enhancement of phosphine distribution over the GRS compared with adjacent regions of Jupiter. It could be argued, however, that the angular resolution of these observations was marginal for this project, so the GRS spectra may have been contaminated with light from the neighboring areas. To rule out this source of ambiguity, we have studied GRS spectra recorded by the Voyager IRIS (Infrared Interferometer Spectrometer) instrument, in both the 5 and 10 micron regions of the spectrum. We used the Voyager temperature profiles and studies of cloud structure in the jovian atmosphere to supplement our investigation of the GRS and the adjacent South Tropical Zone (Kunde *et al.* 1982).

2. DESCRIPTION OF CALCULATIONS

Using Voyager 1 IRIS data, we selected data for the GRS, and the South Tropical Zone (STZ) at the same latitude as the GRS. We obtained 148 data points for the GRS between latitudes -15° and 30°, and longitudes 60° and 90°, and 176° data points for the STZ between latitudes -15° and -30° and longitudes 0° and 360°.

In Figure 1, a flux ratio of summed spectra of the GRS and STZ is shown. Two deep features in the $200 - 800cm^{-1}$ spectral range are caused by the S(0) and S(1) pressure-induced absorption lines of H_2. Between 800 and $1100cm^{-1}$, NH_3 provides the dominant opacity and the flux ratio spectrum is in absorption. These absorption features in the flux ratio spectrum indicate that the tropospheric temperature of the GRS is lower than that of the STZ. On the other hand, the emission feature of the ν_4 band of CH_4 in the $1200 - 1400cm^{-1}$ spectral range indicates that the stratospheric temperature of the GRS is warmer than that of the STZ. We also found that the overall brightness temperature of the 5 micron continuum of the GRS is almost the same as that of the STZ. However, the 5 micron brightness at the rim of the GRS is greater than the brightness at the center. Generally, the rim of the GRS is warmer than the center except in the $1200 - 1400cm^{-1}$ spectral range. This suggests that the structure (dynamics) of the GRS is distinctly different in the troposphere and the stratosphere.

Table 1. Molecular Band Models.

Molecule	Band	Band Intensity	Molecular Parameter	Temperature dependent hydrogen broadening line width ($cm^{-1}atm^{-1}$)
CH_4	ν_4	Orton & Robiette (1980)	Orton & Robiette (1980)	$0.075\ (300/T)^{0.5}$
CH_3D	ν_6	Varanasi & Kim (1981)	Pinkley *et al.* (1977)	$0.075\ (300/T)^{0.5}$
NH_3	ν_2	Taylor (1973b)	Taylor (1973b)	$0.075\ (295/T)^{5/6}$
PH_3	ν_4	Goldman *et al.* (1980)	Goldman *et al.* (1980)	$0.075\ (300/T)^{5/6}$

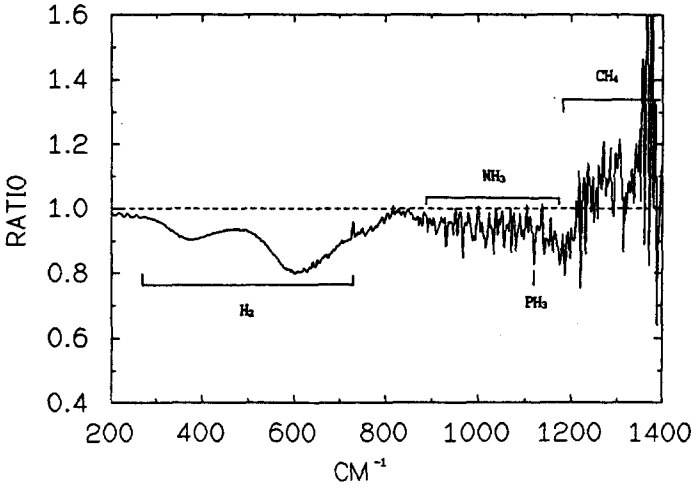

Figure 1. A ratio of summed spectra of the GRS and STZ as recorded by IRIS. The dominant features are H_2 absorption ($200 - 800cm^{-1}$), NH_3 absorption ($1100 - 1200cm^{-1}$), and CH_4 emission ($1200 - 1400cm^{-1}$).

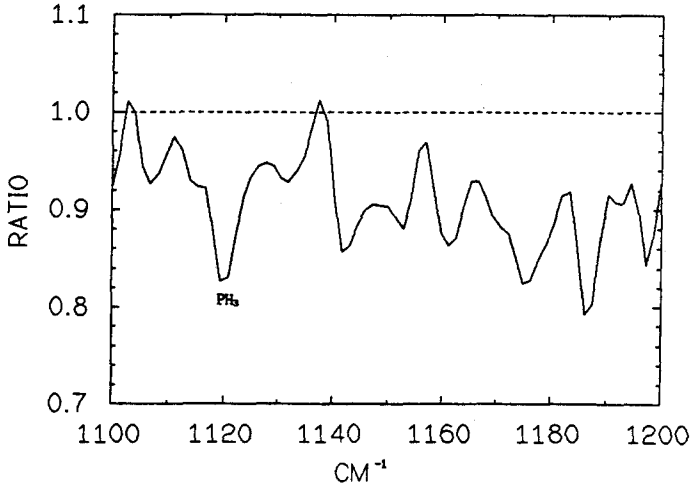

Figure 2. The $1100 - 1200cm^{-1}$ region of the flux ratio in Figure 1 enlarged to show the PH_3 absorption at $1120cm^{-1}$.

In order to derive a PH_3 mixing ratio in the GRS, we used an absorption feature of PH_3 at $1120cm^{-1}$. We chose this feature because in this spectral range strong NH_3 and CH_4 opacities are relatively small and thus the absorption of a minor constituent like PH_3 is easily revealed. In Figure 2, an enlargement of the $1100 - 1200cm^{-1}$ spectral range of Fig. 1 is shown. The PH_3 feature at $1120cm^{-1}$ shown as an absorption in the flux ratio spectrum. This absorption may be explained by either an enhanced PH_3 mixing ratio in the GRS or a lower tropospheric temperature of the GRS compared with that of the STZ. In order to resolve this ambiguity, we first derived thermal profiles of the GRS and the STZ using the S(0) and S(1) lines of H_2. The derived thermal structure of the STZ is very close to that of Marten *et al.*'s (1981) cold model for the jovian atmosphere. The temperature near the tropopause of the GRS is found to be about $5°K$ colder than that of the STZ. Using the derived thermal structures we made synthetic spectra of the $1100 - 1200cm^{-1}$ spectral regions of the GRS and the STZ. We included NH_3, PH_3, CH_3D, and CH_4. Molecular band parameters used in this paper are listed in Table 1.

We found that including all the bands from the 4 molecules just listed, plus the H_2 opacities is not enough to reproduce the continua in the $1100 - 1200cm^{-1}$ spectral ranges of the GRS and the STZ. This is consistent with the results of Marten *et al.* (1981). These authors introduced NH_3 ice particles with a radius greater than 30 microns to suppress the high continua of their pure molecular bands. They also found that introducing an opaque cloud deck is not adequate to explain the whole continuum in the $800 - 1200cm^{-1}$ spectral range of the IRIS data. Following Marten *et al.* (1981), we introduced NH_3 ice haze layers at the pressure level between 0.65 and 0.35 atmospheres. We used the Mie single scattering formulation to calculate the opacities of the NH_3 ice particles with the optical constants for NH_3 ice reported by Taylor (1973a).

A line-by-line radiative transfer program of Kim *et al.* (1995) was used to produce model spectra. Voyager profiles were used for the line shapes of the vibration-rotation bands of the molecules with a frequency step size of $0.005cm^{-1}$. For the 'Lorentz cutoff', we used 300 times the pressure widths or 300 times the Doppler width, depending which was larger.

The best fit of the GRS spectrum is shown in Figure 3. The derived mixing ratios of NH_3, PH_3, CH_4, and CH_3D for the GRS and the STZ are summarized in Table 2. We found that the derived NH_3 distributions of the GRS and the STZ are similar, and consistent with that of Marten *et al.*'s (1981) cold model. We also found that the CH_3D and CH_4 mixing ratios in the GRS are not different from

Table 2. Derived Mixing Ratios.

Species	[Species]/[H_2] GRS	[Species]/[H_2] STZ	Remarks
CH_4	$2.5 +/- 0.5 \times 10^{-3}$	$2.5 +/- 0.5 \times 10^{-3}$	
CH_3D	$4.3 +/- 1.0 \times 10^{-7}$	$4.3 +/- 1.0 \times 10^{-7}$	
NH_3	$1.5 +/- 0.3 \times 10^{-4}$	$1.5 +/- 0.3 \times 10^{-4}$	Below 650 mbar level
PH_3	$4.4 +/- 1.0 \times 10^{-7}$	$4.4 +/- 1.0 \times 10^{-7}$	Below 140 mbar level
NH_3 ice particle optical depth	0.70	0.58	

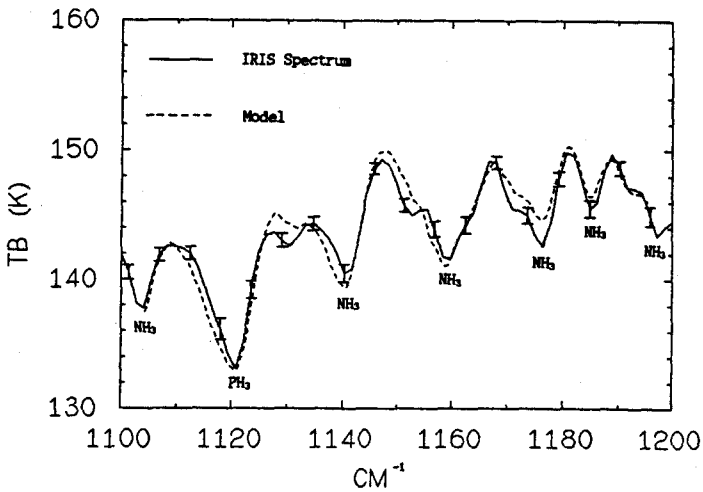

Figure 3. The brightness temperature spectrum of the GRS as observed by IRIS (solid line) and as modelled (dashed line).

those in the equatorial region (Knacke *et al.* 1982) and the STZ. The largest uncertainties in the mixing ratios come from uncertain continuum opacity and the error bars of the IRIS data. Within these uncertainties, the PH_3 abundance over the GRS is the same as that of the STZ and the difference of the two abundances does not exceed 40% of the PH_3 mixing ratio of the GRS. This result agrees with the earlier conclusion of Tokunaga *et al.* (1980), although they used a different thermal structure for the GRS and introduced opaque cloud decks instead of NH_3 ice particles.

3. DISCUSSION

To see whether or not this result is really in disagreement with the predictions of Prinn & Lewis (1975), we must compare the temperature profile and phosphine distribution deduced from these observations with their model calculations. This comparison is illustrated in Figure 4. The phosphine distributions postulated by Prinn & Lewis (1975) are indicated by the dashed lines. The solid lines predict the mass density of red phosphorous particles. The lines labeled I refer to the average planetary conditions, while II anticipates condition over the GRS. The results obtained by the present analysis are given as a dot-dashed line labeled "this work". They are additionally compared with the results of Kunde *et al.* (1982) for the North Equatorial Belt (NEB).

It is apparent from this figure (in agreement with Figure 3) that the levels in the atmosphere we are probing in the region of $1120cm^{-1}$ where we fit the PH_3 feature with our model spectrum are significantly lower than the region of the atmosphere in which the greatest enhancement of phosphine is predicted. We are sampling the atmosphere just at the levels (pressure = 100 - 600 mbar) where the predicted mixing ratios are indistinguishable from each other. Nevertheless, the deviation of the

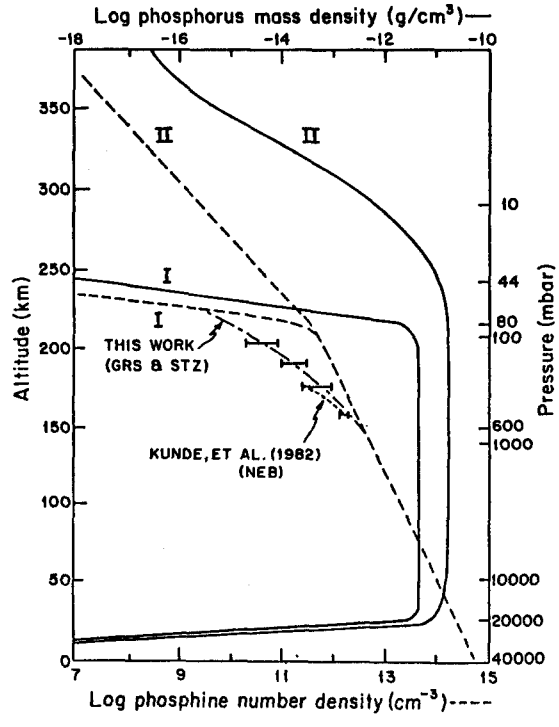

Figure 4. The model distributions of PH_3 on Jupiter from Prinn & Lewis (1975). The lines labeled I refer to the average planetary conditions, while II anticipates conditions over the GRS. The solid lines predict the mass density of red phosphorous particles (top scale) and the dashed lines give the PH_3 number density (bottom scale). The Voyager results are given by the short dashed line (Kunde *et al.* 1982) and the dot-dashed line (this work).

observed from the predicted values is already apparent in the upper troposphere. Phosphine is not being brought to the upper atmosphere as efficiently as was presumed, either in the GRS or the NEB. There is an indication of slightly greater phosphine abundance above the GRS than the NEB, but since the same could be said for the STZ, the effect if real, may be latitudinal rather than specific to the GRS.

To sample still higher levels in the atmosphere we must move to a different part of the spectrum, and here the UV seems especially attractive since the "color" of the GRS is evident as short as 2400 Å (Hord *et al.* 1979). This is an excellent project for the Space Telescope, but it is not obvious PH_3 will be detectable in the UV, because of absorption by NH_3 (Owen *et al.* 1980, Wagener *et al.* 1985). Yet another possibility is to search in the infrared for P_2H_4, as suggested by Ferris & Benson (1981) who showed that this compound is an important intermediary in the photolytic production of P_4 from PH_3.

Meanwhile, there are other aspects of the phosphorous model than can be tested by the IRIS

data. Noy *et al.* (1982) have found that laboratory simulations of jovian photochemistry lead to the production of yellow, not red particles. A red color can still be produced if the particles are the right size (0.05 microns), have an optical depth near unity at 4000 Å, and lie above a white surface. Noy *et al.* (1982) find that these constraints are consistent with an eddy diffusion coefficient on the order of $10^6 cm^2 sec^{-1}$ as postulated by Prinn & Lewis (1975). An independent study of the eddy diffusion coefficients within the GRS is obtainable from a study of GRS dynamics. Such a study was carried out by Conrath *et al.* (1981) who find evidence for an eddy diffusion coefficient on the order of $10^4 cm^2 sec^{-1}$. A value 100 times larger seems very unlikely except in small disturbances (Conrath 1993).

We conclude from these points of inquiry that the IRIS data do not lend support to the idea that the color of the GRS is caused by red phosphorous. On the other hand, this possibility is not completely ruled out, nor is an alternatively suggested by the data. Additional spectroscopic observations are required to search for local traces of intermediate compounds or a specific spectral signature of the red material itself. Neither approach has been successful thus far.

ACKNOWLEDGEMENTS: This research was supported by the Korea Science & Engineering Foundation.

REFERENCES

Conrath, B. J. 1993, Private communication
Conrath, B. J., Flasar, F., Pirraglia, J., Gierasch, P. & Hunt, G. 1981, JGR, 86, 8769
Ferris, J. & Benson, R. 1981, J. Amer. Chem. Soc., 103, 1922
Goldman, A., Cook, G. & Bonomo, F. 1980, JQSRT, 24, 211
Hord, C., West, R., Simmons, K., Coffeen, D., Sato, M., Lane, A. & Bergstralh, J. 1979, Science, 206, 956
Huntress, W. & Anicich, V. 1984, BAAS, 16, 648
Khare, B. & Sagan, C. 1973, Icarus, 20, 311
Kim, S., Kim, Y., Maillard, J.-P., Caldwell, J. & Bjoraker, G. 1995, Icarus, 116, 423
Knacke, R., Kim, S., Ridgway, S. & Tokunaga, A. 1982, ApJ, 262, 388
Kunde, V., Hanel, R., Maguire, W., Gautier, D., Baluteau, J., Marten, A., Chedin, A., Husson, N. & Scott, N. 1982, ApJ, 263, 443
Lewis, J. & Prinn, R. 1970, Science, 169, 472
Marten, A., Ronan, D., Baluteau, J., Guatier, D., Conrath, B., Hanel, R., Kunde, V., Samuelson, R., Chedin, A. & Scott, N. 1981, Icarus, 46, 233
Moroz, V. & Cruikshank, D. 1969, J. Atmos. Sci., 26, 865
Noy, N., Podolak, M. & Bar-Nun, A. 1981, JGR, 86, 11985
Orton, G. & Robiette, A. 1980, JQSRT, 24, 81
Owen, T., Caldwell, J., Rivolo, A., Moore, V., Lane, A., Sagan, C., Hunt, G. & Ponnamperuma, C. 1980, ApJ, 236, L39
Owen, T. & Mason, H. 1969, J. Atmos. Sci., 26, 870
Pinkley, L., Rao, N., Tarrago, G., Possigue, G. & Dang-Nhu, M. 1977, J. Mol. Spec., 68, 195

Prinn, R. & Lewis, J. 1975, Science, 190, 274
Ridgway, S., Larson, H. & Fink, U. 1976, in Jupiter, The infrared spectrum of Jupiter, ed. T. Gehrels (Univ. of Arizona Press: Arizona), p.384
Taylor, F. 1973a, J. Atmos. Sci., 30, 677
Taylor, F. 1973b, JQSRT, 13, 1181
Tokunaga, A., Knacke, R. & Ridgway, S. 1980, Icarus, 44, 93
Varanasi, P. & Kim, S. 1981, JQSRT, 25, 301
Wagener, R., Caldwell, J., Owen, T., Kim, S., Encrenaz, Th. & Combes, M. 1985, Icarus, 63, 222
West, R. & Tomasko, M. 1980, Icarus, 41, 278
Woeller, F. & Ponnamperuma, C. 1969, Icarus, 10, 386